Crystalline bis(η^5-cyclopentadienyl)bis(benzoato/carboxylato)titanium(IV) precursor-directed route to functional titanium dioxide nanomaterials

TUSHAR S. BASU BAUL, *,[a] RAJESH MANNE,[a], EDWARD R. T. TIEKINK,,[b]**

[a]Centre for Advanced Studies in Chemistry, North-Eastern Hill University, NEHU Permanent Campus, Umshing, Shillong 793 022, India

[b]Research Centre for Crystalline Materials, School of Science and Technology, Sunway University, 47500 Bandar Sunway, Selangor Darul Ehsan, Malaysia

Abstract

Five titanocene(IV) carboxylates of the general formula $Cp_2Ti(O_2CR)_2$ viz., [Ti(η^5-C_5H_5)$_2$($O_2CC_6H_5$-4-CH_3)$_2$] (**1**), [Ti(η^5-C_5H_5)$_2$($O_2CC_4H_3$-2-O)$_2$] (**2**), [Ti(η^5-C_5H_5)$_2$($O_2CC_4H_3$-3-O)$_2$] (**3**), [Ti(η^5-C_5H_5)$_2$($O_2CC(CH_3)_3$)$_2$] (**4**) and [Ti(η^5-C_5H_5)$_2$($O_2C(CH)C(CH_3)_3$)$_2$] (**5**) have been synthesized. All the titanocene(IV) carboxylates have been characterized by IR, ^{1}H and ^{13}C NMR spectroscopic techniques, and the crystal and molecular structures of **1**-**5** have been determined by single crystal X-ray crystallography. The structures present similar features with monodentate carboxylate ligands and tetrahedral Ti centres, assuming the each Cp ring occupies one position only. The differences in the structures relate primarily to the relative orientations of the carboxylate ligands. In the molecular packing, non-conventional Cp-C–H···O(carbonyl) hydrogen bonds are observed in each case and lead to supramolecular chains in each of **1**, **4** and **5**. In **2**, the 2-furyl-O atoms also participate in C–H···O interactions leading to a two-dimensional array. Finally, in **3**, a two-dimensional array arises as a result of Cp-C–H···O(carbonyl) and 3-furyl-C–H···O(carbonyl) interactions. As representative example, compound **3** was used as starting material for the synthesis of TiO_2 nanoparticles.

An effective and simple wet-chemical method involving calcination and ultrasonication route has been suggested for obtaining pure anatase TiO_2 NPs, which were confirmed from the powder XRD and imaging techniques such as SEM, TEM and EDS.

Keywords: Benzoate, Carboxylate, Titanocene complexes, Crystal structure, TiO_2 nanoparticles, Anatase

---

* Corresponding author. *E-mail address*: basubaul@nehu.ac.in, basubaulchem@gmail.com (T. S. Basu Baul).

** Additional corresponding author. *E-mail: edwardt@sunway.edu.my*

1. Introduction

Titanium(IV) complexes form a major class of organometallic and coordination compounds which display effective and tuneable reactivities [1-3]. These compounds are also marked as effective catalysts [4-8], have featured in metallo-supramolecular chemistry [9,10] and have applications in medicinal and bioinorganic chemistry [11,12]. Among the latter, Cp_2TiCl_2 was investigated as an anti-cancer drug, based on the presence of the dichloride entity under the assumption its mode of biological action would be closely aligned with that of cisplatin, [cis-$PtCl_2(NH_3)_2$]. However, Cp_2TiCl_2 did not advance in clinical trials owing to its low efficacy against the examined tumours and because of its inherent limitations such as poor water-solubility and instability, the latter due to extensive hydrolysis [13-15]. In spite of the unsatisfactory results of the phase II clinical trials, various researchers have continued investigations into titanium-based drugs, sparking interest in the synthesis of second-generation titanocene and titanium(IV) complexes with anti-cancer properties [16-24]. Recently, a novel biocompatible strategy of drug delivery, employing silica-based materials loaded with titanium compounds for nanodrug delivery systems, exhibited promising results and is under further development [25].

On the other hand, the generation of nanostructured materials with control over both the crystal phase and the morphology still remains a challenge owing to the rapid hydrolysis of titanium tetrachloride and titanium alkoxide or aryloxide species, which are widely used as titanium precursors [26]. In this context, considerable attention has been paid to monitor their hydrolysis using dihydric alcohols, chelating carboxylic acids or other additives [27-29]. Extensive attempts have also been made to develop appropriate titanium precursors for the preparation TiO_2 with tuneable phases and structures using simple experimental procedures [30]. A one-pot and template-free strategy for synthesizing hollow TiO_2 nanostructures using Cp_2TiCl_2 as the titanium source has been described [31].

Although the rich chemistry and diverse biological properties of titanocene and titanium(IV) based compounds have been thoroughly explored, the number of isolated and structurally characterized titanocene carboxylates/benzoates is relatively small [32-38]. Being intrigued by the scarcity of structural reports detailing the coordination chemistry of titanocene carboxylates, the present work aimed to synthesize and investigate the structures of a series of these compounds. For this purpose, three different types of simple carboxylate ligand precursors, namely (i) 4-methylbenzoate (ii) isomeric 2- and 3-furan carboxylates and (iii) 2,2-dimethylpropanoate and 3,3-dimethylbutanoate were selected, which are aromatic, heterocyclic and aliphatic in character, respectively. It is noted that these short chain carboxylic acids are soluble in water, commercially available, inexpensive, less toxic and insensitive to humidity. As part of a research program aimed at the determination of structures arising from the coordination of such ligands, five titanocene(IV) compounds of the general formula $Cp_2Ti(O_2CR)_2$ have been synthesized (**1**-**5**) and their crystal and molecular structures determined by single crystal X-ray crystallography. As a representative case, crystalline titanocene carboxylate, i.e. $[Ti(\eta^5\text{-}C_5H_5)_2(O_2CC_4H_3\text{-}3\text{-}O)_2]$ (**3**), has been explored as a titanium precursor for the synthesis of TiO_2 nanomaterials by fine-tuning the experimental conditions involved in the wet-chemical synthesis.

2. Experimental

2.1. Materials and measurements

Bis(η^5-cyclopentadienyl)titanium(IV) dichloride, pivalic acid, *t*-butyl acetic acid, *p*-toluic acid (Merck), 2-furoic acid and 3-furoic acid (SRL) were used without further purification. The solvents used in the reactions were of AR grade and were dried using standard procedures. Benzene, toluene, hexane and THF were distilled from benzophenone/sodium while methanol was distilled over activated magnesium. Triethylamine was dried over

calcium hydride and distilled. All manipulations were performed using standard Schlenk anaerobic lines in an atmosphere of dry dinitrogen or argon, unless otherwise stated.

Melting points were measured using a Büchi M-560 melting point apparatus and are uncorrected. IR spectra in the range 4000-400 cm^{-1} were obtained on a Perkin Elmer Spectrum BX series FT-IR spectrophotometer with samples investigated as KBr discs. ^{1}H and ^{13}C NMR spectra were recorded on a Bruker AMX 400 spectrometer at 400.13 and 100.62 MHz, respectively. ^{1}H and ^{13}C chemical shifts were referenced to Me_4Si and $CDCl_3$ set at 0.00 and 77.0 ppm, respectively.

For the nanomaterial work, the calcination of **3** was carried out in a Revotek GMP muffle furnace at a heating rate of 10 °C min^{-1} from 25 to 800 °C. Ultrasound irradiations were accomplished with a Sonics VCX 750 instrument equipped with a high intensity ultrasonic probe (13 mm tip diameter; Ti-horn, 20 kHz, 750 Watt) that was immersed directly into the reaction mixture. For the analysis of the TiO_2 nanoparticles, powder X-ray diffraction (PXRD) studies were carried out on a PAN analytical Advanced Bragg Brentano X-ray powder diffractometer using Cu*K*α radiation (λ = 0.154178 nm) with a scanning rate of 0.020 s^{-1} in the 2θ range 10-80°. Scanning Electron Microscope (SEM) from TESCAN (VEGA) with magnification range from ×30 to ×3,00,000, accelerating voltage from 0.3 to 30 kV and with a resolution of 3.5 nm @ 25 kV high vacuum mode, was used. A very dilute solution of as-synthesized nanopowder in isopropanol was sonicated and drops casted on smooth surface of aluminum foil, which was dried over a hot air oven and used for SEM studies. Transmission Electron Microscope (TEM) with Energy Dispersive Spectroscopy (EDS) from JEOL (JEM-2100) with magnification range from ×50 to x1,500,000, accelerating voltage from 60-200 kV in 50 V steps and a High resolution CCD camera 2.672 x 2.672 K, was used. A very dilute solution of as-synthesized nanopowder in isopropanol was sonicated and drops casted on carbon coated copper grid, which was dried over a hot air oven and used for TEM

studies. The EDS spectrum was obtained at an acceleration voltage of 20 keV and collected for 50 s. Mapping was accomplished using pseudo-colors to represent the two-dimensional spatial distribution of energy emissions from the chemical elements present in the sample. A Leica Microscope (M125 C), with illumination system MCI5000, along with a digital fire wire camera DFC295 and transmitted light base with a polarising rotating stage were used for the analysis of the surface textures of the bulk materials.

2.2. Synthesis of pro-ligands

2.2.1. Synthesis of sodium 4-methylbenzoate. Freshly polished sodium metal (0.163 g, 7.08 mmol) was added to anhydrous methanol (10 mL) under an argon atmosphere and stirred for 30 min. A methanolic solution (15 mL) of 4-methylbenzoic acid (0.963 g, 7.08 mmol) was added to the stirred solution of sodium methoxide and the stirring was continued for 2 h. The resulting clear solution was filtered, and the filtrate was concentrated to dryness and kept under vaccum. The dried solid was washed successively with anhydrous hexane and anhydrous benzene to remove excess of sodium methoxide and 4-methylbenzoic acid, respectively, and dried in vacuo. The dried sodium 4-methylbenzoate was heated to reflux in anhydrous toluene using a Dean Stark apparatus to remove traces of moisture. The toluene was removed on a rotary evaporator and the product was dried in vacuo. Yield: 0.66 g, 55 %. M. p.: > 350 ˚C. IR absorption (cm^{-1}): 1637, 1594, 1550, 1453, 1416, 1098, 761.

2.2.2. Synthesis of sodium furan-2-carboxylate. An analogous method to that used for the preparation of sodium 4-methylbenzoate was followed using sodium (0.1025 g, 4.45 mmol) and furan-2-carboxylic acid (0.5 g, 4.461 mmol). Yield: 0.54 g, 75 %. M. p.: > 350 ˚C. IR absorption (cm^{-1}): 1593, 1567, 1484, 1426, 1376, 1190, 1143, 1017, 1009, 926, 884, 809, 790, 725, 608.

2.3. Preparation of titanocene compounds 1-5

2.3.1. Synthesis of Bis(η^5-cyclopentadienyl)bis(4-methylbenzoato-κ*O*)titanium(IV) (1). A freshly prepared solution of titanocene dichloride (0.25g, 1.004 mmol) in anhydrous benzene (15 mL) was added to a stirred suspension of sodium 4-methylbenzoate (0.396 g, 2.504 mmol) in anhydrous benzene (15 mL) and the stirring was continued at 40 ˚C for 4 h. During reaction, the colour of the reaction mixture changes from blood-red to bright-orange. The orange solution was filtered through a frit covered with pre-dried neutral silica (1 cm layer, mesh size 100-200) and eluted further with anhydrous benzene (3 x 0.5 mL). The clear filtrate was concentrated using a rotary evaporator to around 5 mL and precipitated with excess of anhydrous hexane. The orange solid was collected on a frit, washed with hexane (2 x 5 mL), dried and recrystallized from anhydrous toluene under ambient conditions to afford orange crystals of 1 at ambient temperature. Yield: 0.27 g, 55 %. M. p.: 176-178 ˚C (dec.) 174-176 ˚C (dec.) [39]. IR absorption (cm^{-1}) 1625 $\nu(OCO)_{asym}$, 1574, 1446, 1335 $\nu(OCO)_{sym}$, 1306, 1289, 1169, 1135, 1020, 808, 756, 611, 570, 467. ^1H NMR ($CDCl_3$): 7.87 (d, J = 8.6 Hz, 4H, H-2/H-6), 7.18 (d, J = 8.6 Hz, 4H, H-3/H-5), 6.54 (s, 10H, C_5H_5), 2.36 (s, 6H, CH_3) ppm. $^{13}C\{^1H\}$ NMR ($CDCl_3$): 172.3 (COO), 142.2 (C-1), 130.9 (C-4), 130.0 (C-2/C-6), 128.9 (C-3/C-5), 118.4 (C_5H_5), 21.6 (CH_3) ppm.

2.3.2. Synthesis of Bis(η^5-cyclopentadienyl)bis(furan-2-carboxylato-κ*O*)titanium(IV) (2).

An analogous method to that used for the preparation of **1** was followed using titanocene dichloride (0.25 g, 1.004 mmol) and sodium furan-2-carboxylate (0.28 g, 2.08 mmol). The yellow solid was collected on a frit, washed with hexane (2 x 5 mL), dried and recrystallized from anhydrous benzene at ambient temperature to afford orange crystals of **2**. Yield: 0.30 g, 65 %. M. p.: 188-190 ˚C (dec.), 182-184 ˚C (dec.) [39]. IR absorption (cm^{-1}): 1646

ν(OCO)$_{asym}$, 1566, 1475, 1395 ν(OCO)$_{sym}$, 1332, 1308, 1230, 1164, 1138, 1015, 822, 765, 567. ^{1}H NMR ($CDCl_3$): 7.50 (urd, 2H, H-4), 7.03 (urd, 2H, H-3), 6.56 (s, 10H, C_5H_5), 6.44 (urd, 2H, H-5) ppm. $^{13}C\{^{1}H\}$ NMR ($CDCl_3$): 164.3 (COO), 147.6 (C-1), 145.3 (C-4), 118.8 (C_5H_5), 116.6 (C-2), 111.6 (C-3) ppm.

2.3.3. Synthesis of Bis(η^5-cyclopentadienyl)bis(furan-3-carboxylato-κ*O*)titanium(IV) (3).

A freshly prepared solution of titanocene dichloride (0.25 g, 1.004 mmol) in anhydrous benzene (15 mL) was added to a stirred solution of furan-3-carboxylic acid (0.225g, 1.99 mmol) in anhydrous benzene (15 mL). Subsequently, a benzene solution (10 mL) of NEt_3 (0.282 mL, 2.008 mmol) was added dropnwise where upon the blood-red solution turns bright-orange along with precipitation of $Et_3N{\cdot}HCl$. The reaction mixture was slowly heated to 40 ˚C and stirring was continued for additional 4 h. The orange solution was filtered through a frit covered with pre-dried neutral silica (1 cm layer, mesh size 100-200) and eluted with anhydrous benzene (3 x 0.5 mL). The clear filtrate was concentrated using a rotary evaporator to around 2 mL and precipitated with an excess of anhydrous hexane. The orange solid was collected on a frit, washed with hexane (2 x 5 mL), dried and recrystallized from anhydrous benzene at ambient temperature to afford orange crystals, which were isolated by filtration. Yield: 0.35 g, 60 %. M. p.: 110-112 ˚C (dec.). IR absorption (cm^{-1}): 1628 ν(OCO)$_{asym}$, 1562, 1504, 1396 ν(OCO)$_{sym}$, 1338, 1314, 1194, 1182, 1150, 1006, 837, 779, 766, 559. ^{1}H NMR ($CDCl_3$): 8.05 (s, 2H, H-2), 7.39 (urd, 2H, H-5), 6.71 (urd, 2H, H-4), 6.52 (s, 10H, C_5H_5), ppm. $^{13}C\{^{1}H\}$ NMR ($CDCl_3$): 168.9 (COO), 149.1 (C-5), 144.0 (C-2), 120.2 (C_5H_5), 118.7 (C-3), 109.8 (C-4) ppm.

2.3.4. Synthesis of **Bis(η^5-cyclopentadienyl)bis(2,2-dimethylpropanoato-κ*O*)titanium(IV) (4).** An analogous method to that used for the preparation of **3** was followed using titanocene dichloride (0.25g, 1.004 mmol) and 2,2-dimethylpropanoic acid (0.204 g, 2.008 mmol). The yellow solid was collected on a frit, washed with chilled hexane (2 x 5 mL), dried and recrystallized from anhydrous benzene under ambient conditions to afford yellow crystals of **4**. Yield: 0.15 g, 45 %. M. p.: 176-178 ˚C (dec.). IR absorption (cm^{-1}): 2905 ν(C-H), 1624 $\nu(OCO)_{asym}$, 1480, 1451, 1430, 1342 $\nu(OCO)_{sym}$, 1297, 1255, 1105, 1079, 806, 728, 698, 684, 575, 485. ^{1}H NMR ($CDCl_3$): 6.37 (s, 10H, C_5H_5), 1.12 (s, 18H, CH_3) ppm. $^{13}C\{^1H\}$ NMR ($CDCl_3$): 184.1 (COO), 117.9 (C_5H_5), 45.7 (C-1), 27.6 (CH_3) ppm.

2.3.5. Synthesis of Bis(η^5-cyclopentadienyl)bis(3,3-dimethylbutanoato-κ*O*)titanium(IV) (5). An analogous method to that used for the preparation of **3** was followed using titanocene dichloride (0.25g, 1.004 mmol) and 3,3-dimethylbutanoic acid (0.233 g, 2.005 mmol). The yellow solid was collected on a frit, washed with chilled hexane (2 x 5 mL), dried and recrystallized from anhydrous benzene at ambient temperature to afford pale-yellow crystals of **5**. In general, crystals of **5** were obtained during first crystallization but the second attempt at crystallization of the same sample using anhydrous benzene invariably led to greasy materials. Yield: 0.15 g, 45 %. M. p.: 156-159 ˚C (dec.). IR absorption (cm^{-1}): 2905 ν(C-H), 1624 $\nu(OCO)_{asym}$, 1430, 1341 $\nu(OCO)_{sym}$, 1296, 1256, 1079, 806, 727, 698, 575, 485. ^{1}H NMR ($CDCl_3$): 6.53 (s, 10H, C_5H_5), 2.17 (s, 4H, H-1), 0.99 (s, 18H, CH_3) ppm. $^{13}C\{^1H\}$ NMR ($CDCl_3$): 178.8 (COO), 120.2 (C_5H_5), 47.7 (C-1), 30.6 (C-2), 29.5 (CH_3) ppm.

2.4. Single crystal X-ray structure determinations of 1–5

Crystals of compounds **1** (toluene) and **2**-**5** (benzene) suitable for single-crystal X-ray diffraction analysis were grown from the respective solutions by slow solvent evaporation at room temperature. Intensity data for compounds **1**-**5** were measured at room temperature on an Agilent Xcalibur Eos Gemini diffractometer equipped with a CCD area detector and graphite-monochromated Mo Kα radiation (λ = 0.71073 Å). Data reduction and empirical absorption corrections, based on a multi-scan technique, were by standard methods [40]. At θ = 25.2 deg., data completeness was 100% in each case. The structures were solved by direct-methods [41] and refined on F^2 with anisotropic displacement parameters and C-bound H atoms in the riding model approximation [42]. A weighting scheme of the form $w = 1/[\sigma^2(F_o^2) + aP^2 + bP]$ where $P = (F_o^2 + 2F_c^2)/3$) was introduced in each case. The structures uniformly featured high displacement parameters, in particular for the cyclopentadienyl (Cp) groups. Despite this deficiency in the data, the structures were determined unambiguously. In the refinement of **2**, the (-2 0 8) reflection was omitted from the final cycles of refinement owing to poor agreement. Crystal data and refinement details are collected in Table 1. The molecular structure diagrams were generated by ORTEP for Windows [43] and the packing diagrams with DIAMOND [44]. Additional data analysis was made with PLATON [45].

2.5. Synthesis of TiO_2 nanoparticles (NPs)

The dried titanocene carboxylate precursor **3** (0.50 g) was dissolved in chloroform (5 mL) and decomposed using a mixture of HNO_3 (5.0 mL) and $HClO_4$ (5 drops) in a conical flask covered with a glass funnel. The flask was heated gently on a hotplate until the solution turned colourless. The process of decomposition was repeated once more to ensure complete oxidation of organic matters. The acid was removed completely on a hotplate with continuous shaking and the flask was allowed to cool to room temperature. Double distilled

water (5 mL) was added in the flask to obtain a suspension of TiO_2, stirred and filtered using Whatman 42 filter paper. The residue was washed with water until neutral pH, washed with acetone and dried overnight at room temperature. The dried mass was transferred to a platinum crucible and gradually heated in a muffle furnace at a rate of 10 °C/min. until the temperature reached 800 °C. The crucible was heated for further 4 h at 800 °C and cooled gradually to room temperature. The weight of TiO_2 was recorded (0.065 g, 75.2 %) and the phase purity was monitored by PXRD.

An aliquot of the calcinated as-synthesized TiO_2 (0.02 g) was suspended in double-distilled water (10 mL) and exposed to high-intensity ultrasound irradiation under ambient conditions for 30 min. to give a uniform white suspension. After cooling to room temperature, the particles were separated by centrifugation at 6000 rpm. The procedure was repeated three times by re-dispersing the sample in isopropanol. Isopropanol was separated by decantation, the TiO_2 residue was dried in hot air oven for 1 h at 120 °C and stored in vacuum. The dried sample was used directly for the measurement of PXRD pattern. For imaging studies, the dried as-synthesized TiO_2 nanopowder was re-dispersed in isopropanol.

3. Results and discussion

3.1. Synthesis and spectroscopic characterization of compounds 1-5

Earlier, Dang et al. [39] reported the synthesis of **1** and **2** but the yields were 40 and 30 %, respectively. In another endeavour, Branham et al. [46] reported the synthesis of **1** using the same reaction precursors which afforded a mixture of at least three components, viz. Cp_2TiCl_2, $Cp_2TiCl(O_2CC_6H_5\text{-}4\text{-}CH_3)]$ and $[Cp_2Ti(O_2CC_6H_5\text{-}4\text{-}CH_3)_2]$, which could not be separated, as evidenced from ^1H NMR spectroscopy. In view of this, the first goal of this work was to prepare titanocene complexes of aromatic, heterocyclic and aliphatic carboxylic acids in higher yields and to crystallize the powder/ microcrystalline materials to obtain X-

ray quality single crystals to enable the determination of their molecular structures and to assess any influence on the structure exerted by carboxylate ligands. In the present investigation, titanocene carboxylates **1** and **2** were synthesized by the reactions of titanocene dichloride with two equivalents of the freshly prepared corresponding sodium 4-methylbenzoate and sodium furan-2-carboxylate in benzene at 40 ˚C under stirring. On the other hand, **3-5** were prepared by the reactions of titanocene dichloride with the respective organic acids, i.e. furan-3-carboxylic acid, 2,2-dimethylpropanoic acid and 3,3-dimethylbutanoic acid, in benzene in the presence of triethylamine in 1:2:2 molar proportions (Scheme 1). A gradual colour change from blood-red to deep-orange was observed during the reactions, and notably, the final yields of orange (**1-3**) or yellow (**4** and **5**) crystals were dependent on the workup conditions applied for the purification and recovery of the crystals. Crystalline samples of the compounds **1-3** can be stored for several months at an inert environment and of these, compounds **2** and **3** were even stable at ambient conditions for months as monitored by examining their physical states, colors, M. p. (dec.) and IR. However, orange color of compound **1** gradually fades to pale yellow and turns powder with time. On the other hand, vacuum stored compounds **4**-**5** turns pasty within two to three days. The compounds were characterized by NMR, IR spectroscopy and by single-crystal X-ray crystallography.

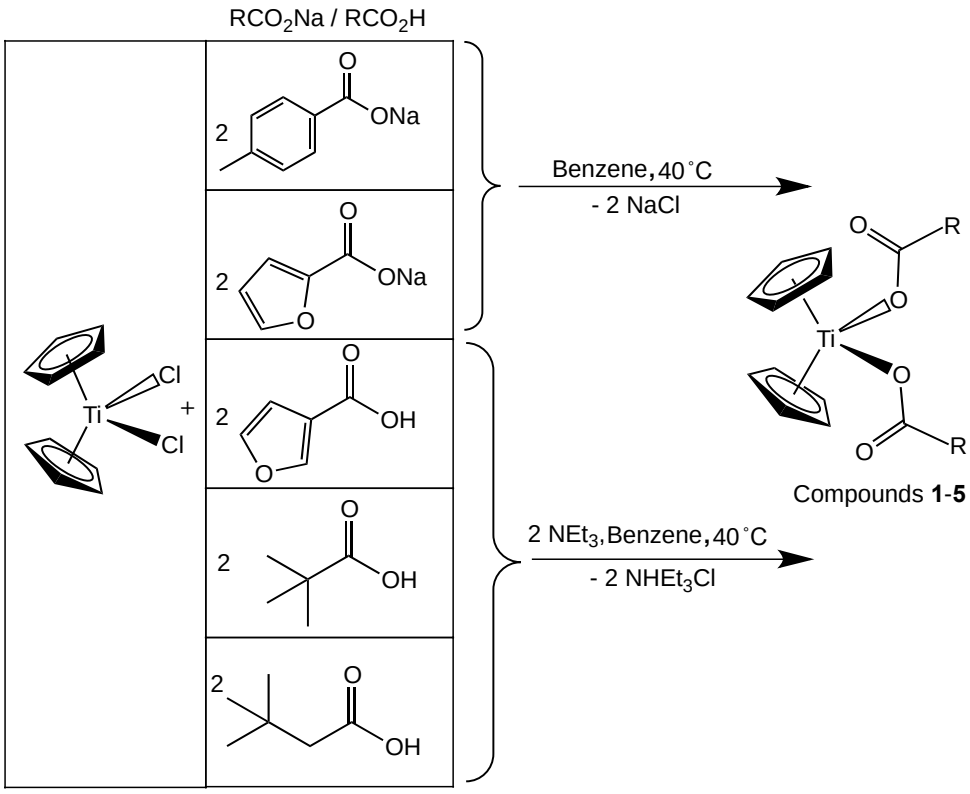

Scheme 1. Schematic representation of the pro-ligands used in the synthesis of titanocene compounds **1**-**5**.

The most relevant IR spectral bands for the synthesized compounds are given in the experimental section. The IR spectra of **1**-**5** show two intense bands in the regions between 1646-1623 and 1396-1335 cm^{-1} corresponding to $\nu(OCO)_{asym}$ and $\nu(OCO)_{sym}$ vibrations, respectively. The observed differences between the asymmetric and symmetric vibrations are greater than 200 cm^{-1}; indicating a monodentate coordination of the carboxylate ligand [47]; this postulate was subsequently confirmed from the results of single crystal X-ray diffraction studies (see Section 3.2). The ^{1}H NMR and $^{13}C\{^{1}H\}$ NMR spectra of compounds **1**-**5** displayed the expected signals due to the carboxylate and Cp ligands. The number of protons calculated from the integration values in the spectra is in agreement with those expected for **1**-**5**. A sharp singlet at around 6.50 ppm was detected for the two Cp rings, which are chemically equivalent. An analogous situation is evident in the ^{13}C NMR whereby a single signal between 117.9 and 120.8 ppm was observed for ten carbon atoms of the two Cp rings. The carboxylate carbonyl-carbon resonances were observed at δ 172.3, 164.3, 168.9, 184.1 and 178.8 ppm for **1**-**5**, respectively.

3.2. Description of the crystal and molecular structures for 1-5

The molecular structures of **1**-**5**, i.e. compounds of general formula $Cp_2Ti(O_2CR)_2$, are illustrated in figure 1 and from this, it is apparent that the structures present quite similar features, at least to a first approximation; selected geometric parameters for the five structures are collated in Table 2. In **1**, the titanium atom is coordinated by two oxygen atoms derived from two monodentate benzoate ligands as the carbonyl-O2 and -O4 atoms are directed away from the titanium atom with the Ti···O2, O4 separations of 3.630(2) and 3.515(2) Å being considerably longer than the Ti–O1, O3 bond lengths of 1.9295(17) and 1.9446(18) Å, respectively. The pseudo tetrahedral coordination geometry about the titanium atom is completed by two η^5-cyclopentadienyl (Cp) anions, each assumed to occupy a single position. The Ti–C(Cp) bond lengths span a narrow

range, i.e. 2.327(5) to 2.351(5) Å for the C17-containing Cp ring and 2.356(4) to 2.384(4) Å for the C22-Cp ring, indicating the bond lengths are experimentally different. The Ti···Cg ring centroid distances of 2.055(3) and 2.0629(18) Å confirms any differences in Ti–C bond lengths are not chemically significant. The tetrahedral angles range from a narrow 90.12(8)°, for O1–Ti–O3, to a broad 132.28(9)°, subtended by the bulky Cp rings. The values of the O1–C1–C2–C3 and O3–C9–C10–C15 torsion angles of -13.1(3) and -11.5(4)°, respectively, indicate twists in the benzoate ligands. Finally, the dihedral angle between the *p*-tolyl rings of 9.05(15)° indicates an almost co-planar relationship between them. Globally, the carbonyl groups are directed towards the region between Cp rings enabling the organic residues to occupy the space to the other side of the molecule, presumably to reduce steric repulsions.

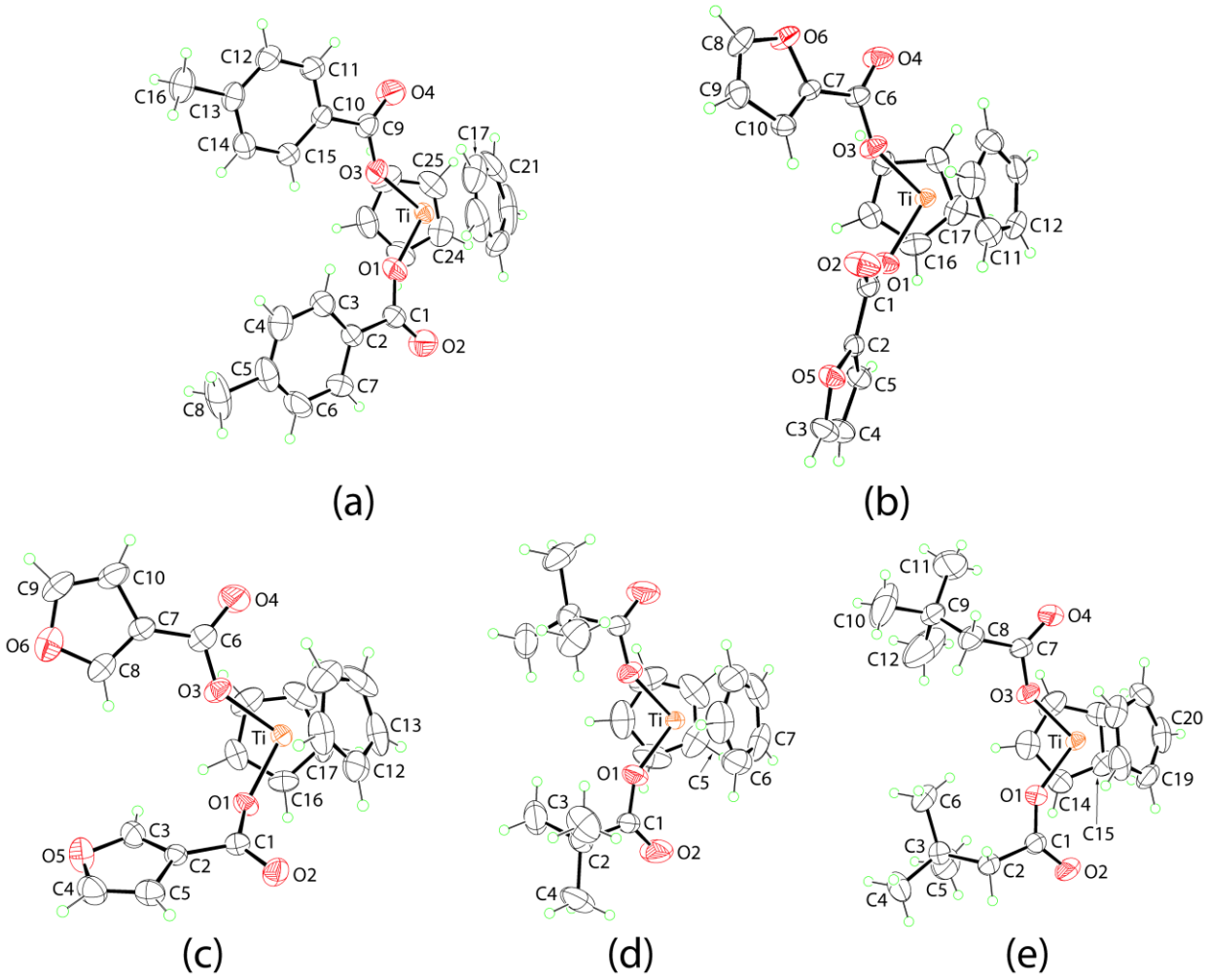

Figure 1. Molecular structures of **1**-**5**: (a) **1**, (b) **2**, (c) **3**, (d) **4** and (e) **5**, showing atom labelling schemes and displacement ellipsoids at the 35% probability level. To reduce congestion, only two labels are shown for the Cp rings in (a)-(c) and (e).

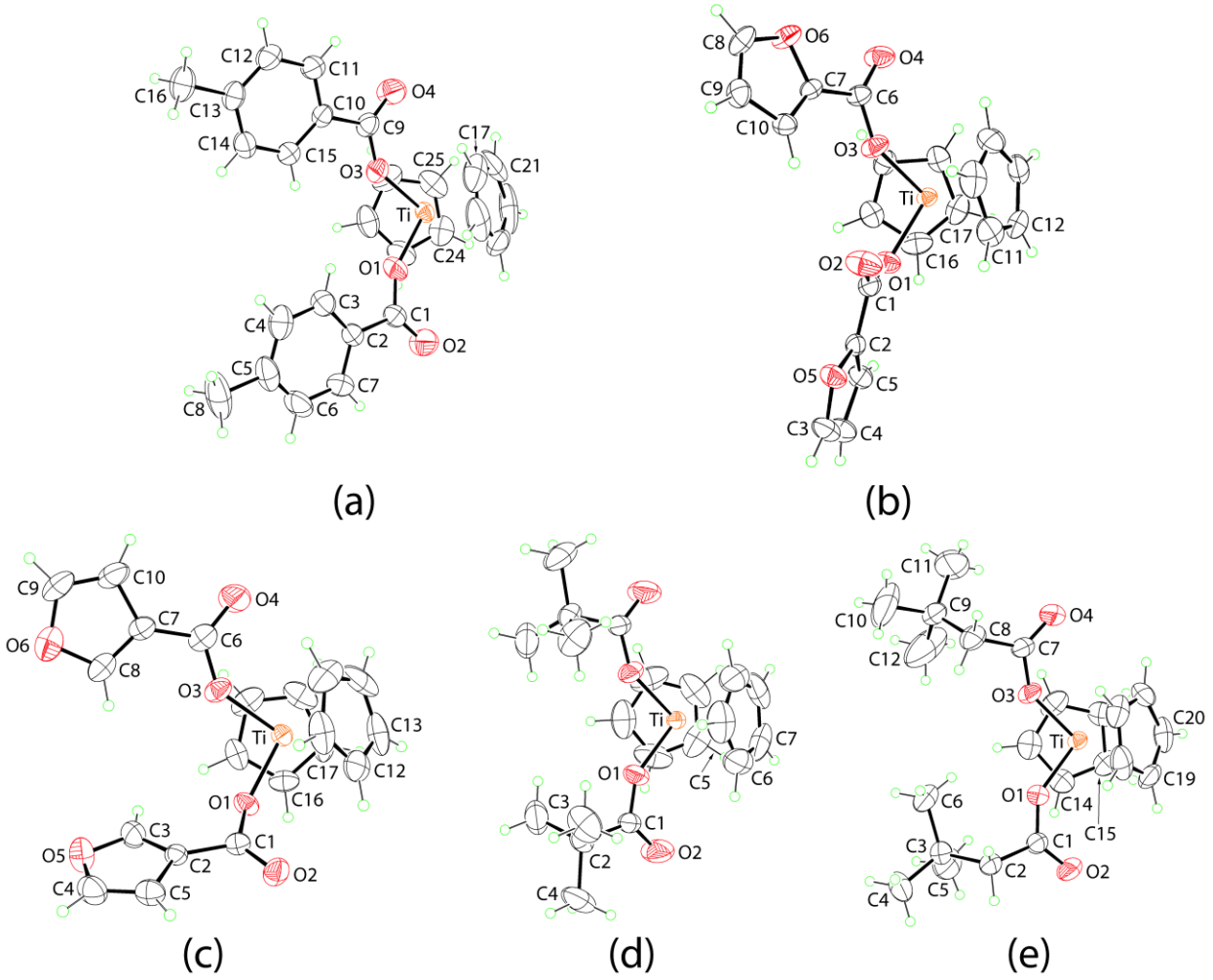

Figure 1. Molecular structures of **1**-**5**: (a) **1**, (b) **2**, (c) **3**, (d) **4** and (e) **5**, showing atom labelling schemes and displacement ellipsoids at the 35% probability level. To reduce congestion, only two labels are shown for the Cp rings in (a)-(c) and (e).

Molecules **2** and **3** contain 2-furyl and 3-furyl substituents, respectively. The Ti–O bond lengths in each of **2** and **3** are experimentally distinct but, not at the 5σ level. Further, the Ti–O bond lengths overlap with the values found in **1**. Similar variations are noted in the Ti–Cg separations. In **2**, the O1-carboxylate anion is planar as seen in the O1–C1–C2–O5 torsion angle of -178.4(3)° but, a small twist is evident in the O3-carboxylate with the O3–C6–C7–O6 torsion angle being -173.6(3)°. Small twists are evident in both carboxylate anions of **3**, viz. O1–C1–C2–C3 is 11.8(6)° and O3–C6–C7–C8 is -7.6(7)°. A difference in the relative orientations of the carboxylate ligands in **1** and **2** is apparent. In **1**, the dihedral angle between the O_2CC residues is 10.38(18)° but, in **2** the equivalent angle is 40.42(15)°, and in **3** this angle is wider at 46.86(16)°. Further, in **2**, there is a splayed relationship between the organic residues of the carboxylate anions, as seen in the dihedral angle of 40.6(2)° between the 2-furyl rings. In **3**, the relative orientation approaches orthogonal with the dihedral angle between 3-furyl rings being 65.6(3)°.

The structure of **4** is remarkable in that it is highly symmetric as opposed to the other structures discussed herein, which lack crystallographically-imposed symmetry. The titanium atom is located on a special site of symmetry, m2m. The $^{-}O_2C$-t-Bu anion is bisected by the mirror plane, and the Cp rings are related across the mirror plane. Further, each Cp ligand lies on a second mirror plane which is orthogonal to the first mentioned mirror plane. As a consequence, the Ti–O bond lengths are identical, as are the Ti–Cg distances. While lacking the molecular symmetry of **4**, the structure of **5** presents many similarities to that of **4**, with experimentally equivalent Ti–O and Ti–Cg separations which, further, are experimentally indistinguishable from the equivalent parameters in **4**. The relative orientations of the carboxylate anions in **4** and **5** approximate those seen in **1**, with the dihedral angles between the O_2CC residues being 0°, from symmetry, and 20.2(2)° in **4** and **5**, respectively.

An evaluation of the crystallographic literature [48] shows there are nearly 20 non-solvated structures conforming to the general formula $Cp_2Ti(O_2CR)_2$. The overwhelming majority of these conform the motif whereby the dihedral angle between the carboxylate O_2CC residues lies in the range 0-20° and both carbonyl-O atoms are orientated towards the region between the Cp rings, i.e. are "syn". The exceptional structure, i.e. $Cp_2Ti(O_2CC_6H_3\text{-}2\text{-}OH\text{-}5\text{-}NO_2)_2$ [49] whereby while being approximately co-planar, the carbonyl-O atoms have an "anti" disposition.

A common feature in the crystals of **1**-**5** is the formation of non-conventional C–H…O hydrogen bonding interactions. As seen from the data collated in Table 3, some of the H…O separations are relatively short and all contacts are relatively directional.

In the crystal of **1**, each of the carbonyl-O2 and -O4 atoms participates in two Cp-C–H···O(carbonyl) interactions as each Cp ring bridges two carbonyl atoms in the molecular packing. This results in the formation of supramolecular 10-membered $\{\ldots O\ldots HCCH\}_2$ synthons and linear chains approximately along [1 $\bar{2}$ 0], figure 2a. In the crystal of **2**, the 2-furyl oxygen atoms come into play and the carbonyl-O2 atom doesn't form interactions within the standard distance criteria of PLATON [45]. In essence, the O5-furyl ring bridges the carbonyl-O4 atom of one molecule and a Cp ring of another. As these interactions extend laterally, a supramolecular layer parallel to [0 0 1] is formed as shown in figure 2b. Curiously, the 3-furyl-oxygen atoms do not participate in significant interactions in the crystal of **3**. As for **1**, both carbonyl-O2 and -O4 atoms participates in two C–H···O interactions. Three of the contacts involve Cp-C–H as donors and one, involving the carbonyl-O2 atom, has 3-furyl-C–H as the donor, Table 3. Again, these interactions extend laterally to form a supramolecular later parallel to [0 0 1], figure 2c. As for **2**, the layer in **3** has a flat topology. In highly symmetric **4**,

each carbonyl-O2 atom participates in two Cp-C–H…O(carbonyl) interactions akin to that observed in the crystal of **1** leading to a similar supramolecular chain and 10-membered $\{\ldots O\ldots HCCH\}_2$ synthons, figure 2d. In the crystal of **5**, each carbonyl-O2 and -O4 atom participates in a single Cp-C–H…O(carbonyl) interaction, Table 3. The result is a supramolecular chain aligned along [0 1 0] linked by a zig-zag arrangement of 12-membered $\{\ldots OCOTiCH\}_2$ synthons. The chain closely resembles those formed in the crystals of **1** and **4** but, lacks the additional Cp-C–H…O(carbonyl) interactions found in the latter, as the putative H…O separations in **5** are greater than 2.85 Å.

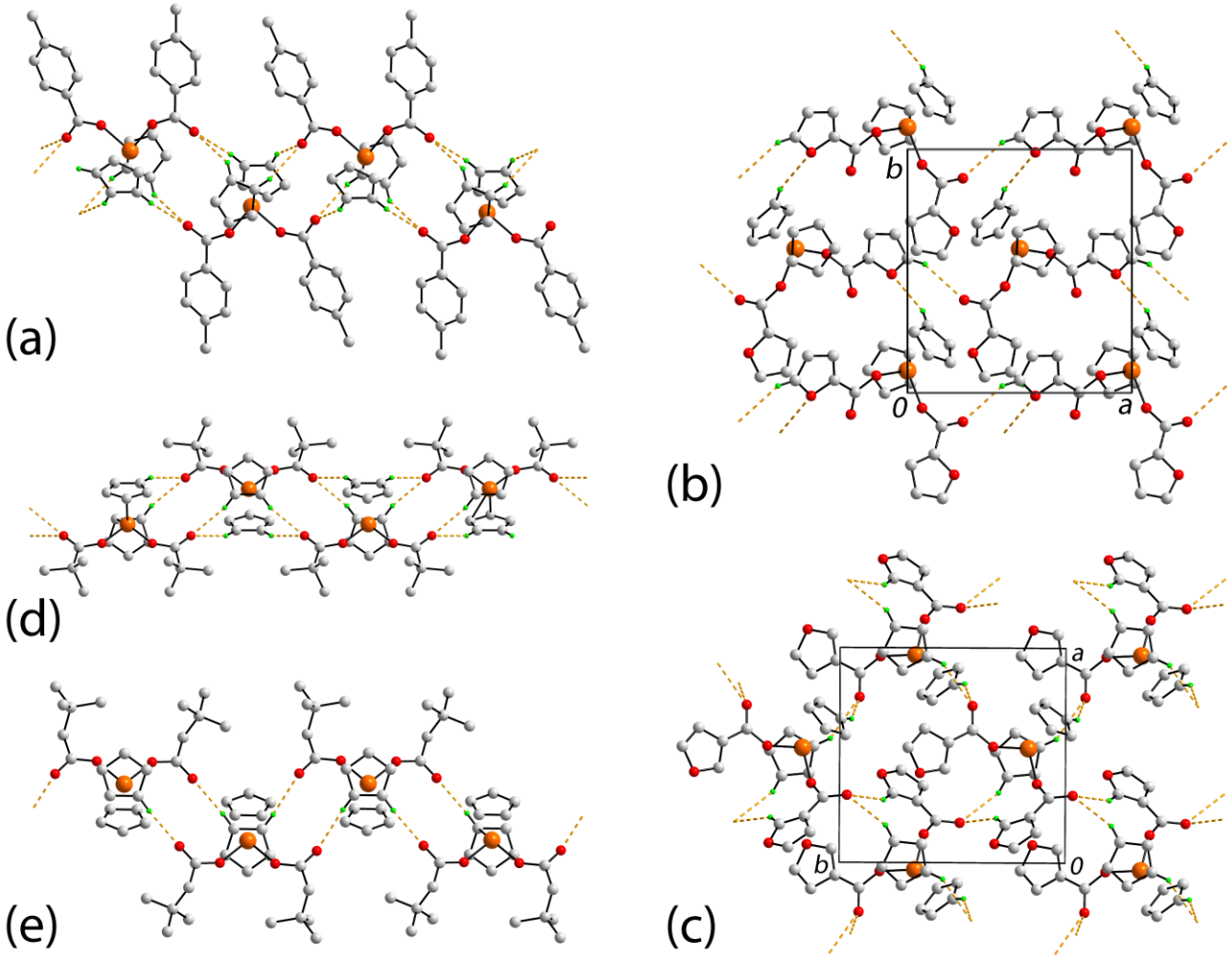

Figure 2. Supramolecular association mediated by C–H···O interactions (shown as orange dashed lines) in the crystals of **1**-**5**: (a) **1**, (b) **2**, (c) **3**, (d) **4** and (e) **5**. Non-participating hydrogen atoms are omitted for reasons of clarity.

3.3. Synthesis and characterization of TiO_2 nanoparticles (NPs)

As indicated in the Introduction, titanium(IV) complexes are actively being investigated, owing to their interesting structural features and applications. Consequently, there has been a tremendous effort placed for the synthesis, properties modifications, and applications of TiO_2 nanomaterials. Currently there are too many variables (both chemical and physical) exist to realistically determine the controlling aspects for the synthetic modifications of the TiO_2 nanoparticles that use $TiCl_4$ or $Ti(OR)_4$ precursors [50]. Although, $Ti(OR)_4$ precursors are often favored for solution routes due to several advantages (high solubility in a variety of solvents, their low decomposition/crystallization temperatures, their ability to crosslink upon exposure to ambient atmosphere) [51] but they are also commonly used in sol-gel, hydrothermal, sonochemical and microwave methods. Commercial small molecule liquid-state $Ti(OR)_4$ precursors i.e. titanium tetraisopropoxide (TTIP) are often too reactive, with ambient humidity forming large complex molecules, in addition to the handing difficulties. Consequently, by comparison, titanium glycerolate was synthesized that too uses titanium ethoxide (readily hydrolysable liquid) and glycerol, and its powder X-ray diffraction pattern is similar to that of crystalline titanium glycolate [52]. On the other hand, structurally characterized titanium glycolate, synthesized from TTIP and ethylene glycol, were transformed into nanostructured TiO_2 with advanced functions [52]. In view of handling difficulties of titanium precursors, a family of chelating titanium carboxylate, e.g., citrates and lactates were developed with features such as molecular structures, solution stability, reactivity and their application possibilities for production of nanomaterials [53,54]. They all can be dissolved and diluted in water at room temperature without formation of visible precipitate and does not require any special precautions as essential for $TiCl_4$ or TTIP precursors [55]. The most attractive feature of the carboxylate

complexes of titanium(IV) is their hydrolytic stability. The *tris*-carboxylato-derivatives, viz., *tris*-lactate $[Ti\{CH_3CHOCOO\}_3]^{2-}$ [56] and *tris*-citrate $[Ti\{OCCOO(CH_2COO)_2\}_3]^{6-}$ [57] anions demonstrated considerable thermal stability at increased pH and temperature under hydrothermal conditions (temperature 180° C) [56] and subsequently produced nanomaterials by combined attempt of sol-gel with metal-organic decomposition. A structurally characterized titanium carboxylate $[Ti\{(CH_3)_3CCOO)_3(CH_3)_3O\}]$ synthesized from 2,2-dimethylpropanoic acid and $Ti(OC(CH_3)_3)_4$ (titanium(IV) tert-butoxide) produced TiO_2 nanowires by electrospinning synthesis under a nitrogen atmosphere, however, the carboxylate compound on exposure to air slowly gets converted to an oxo complex [58]. To overcome such physical and chemical limitations, a series of titanocene(IV) carboxylates were synthesized. Having now the availability of a well-characterized series of tetrahedral titanocene carboxylates (**1**-**5**), it was thought of interest to evaluate the use of these compounds as a titanium source for the generation of nano-structured materials. As a representative example, $[Ti(\eta^5\text{-}C_5H_5)_2(O_2CC_4H_3\text{-}2\text{-}O)_2]$ (**3**) was selected as a precursor for TiO_2 nanoparticles whereby TiO_2 NPs have been synthesized by an effective and simple wet-chemical method (see Supplementary Material figures S1a and S1b). A three-step procedure was applied. The first step involves the decomposition of the metal-organic precursor using a mixture of concentrated nitric acid and perchloric acid (Note: Care in handling of perchloric acid should be exercised) that lead to the formation of a TiO_2 suspension. The second and third steps involve the calcination of TiO_2 suspension (see Supplementary Material figure. S1c); followed by ultrasonication of calcinated TiO_2 (see Supplementary Material figure S1d), affording a TiO_2 nanopowder. This was characterized by PXRD and imaging techniques such as SEM and TEM. The X-ray diffractograms of the as-synthesized TiO_2 nanopowder annealed at (i) 400 °C (ii) 600 °C and (iii) 800 °C are illustrated in Supplementary Material

figure S2. As can be seen in figure S2, a thermal treatment was necessary to stabilize the nanoparticles and the X-ray diffraction pattern for the TiO_2 sample annealed at 800 °C for 4 h indicates the complete formation of a pure anatase phase [59], as the observed PXRD peaks are in very good agreement with those of the pure anatase structure (JCPDS Card No. 21-1272).

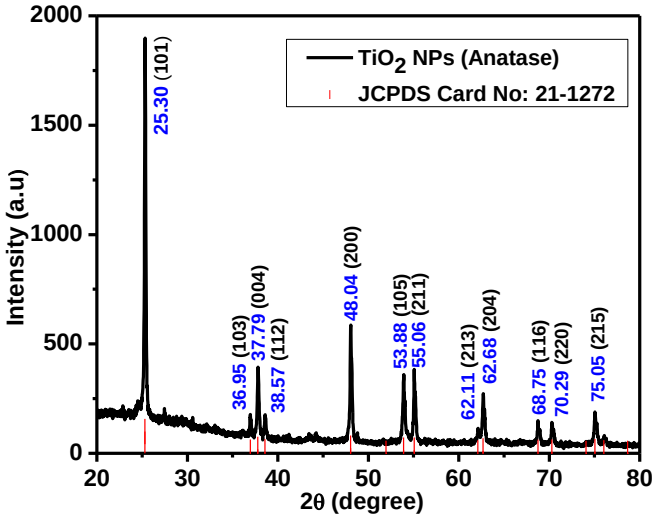

Figure 3. PXRD pattern of as-synthesized TiO_2 nanopowder annealed at 800 °C.

To examine the microstructures of the as-synthesized TiO_2 nanopowder, SEM images were recorded (figure 4a), revealing a uniform distribution of softly agglomerated TiO_2 nanoclustures. The presence of protrusions and pits between nanoparticles are also distinguishable. The TEM image reveals that the particles are rectangular and variable in size. Agglomeration of the deposited particles is also evident (figure 4b). At higher magnification, lattice fringes were observed in as-synthesized particles as shown in Supplementary Material figure S2b. Particles also have a larger surface area, which is also expected especially when the synthesis is carried out in an aqueous medium. The average particle size ranges from 50-60 nm with a slight variation in thickness.

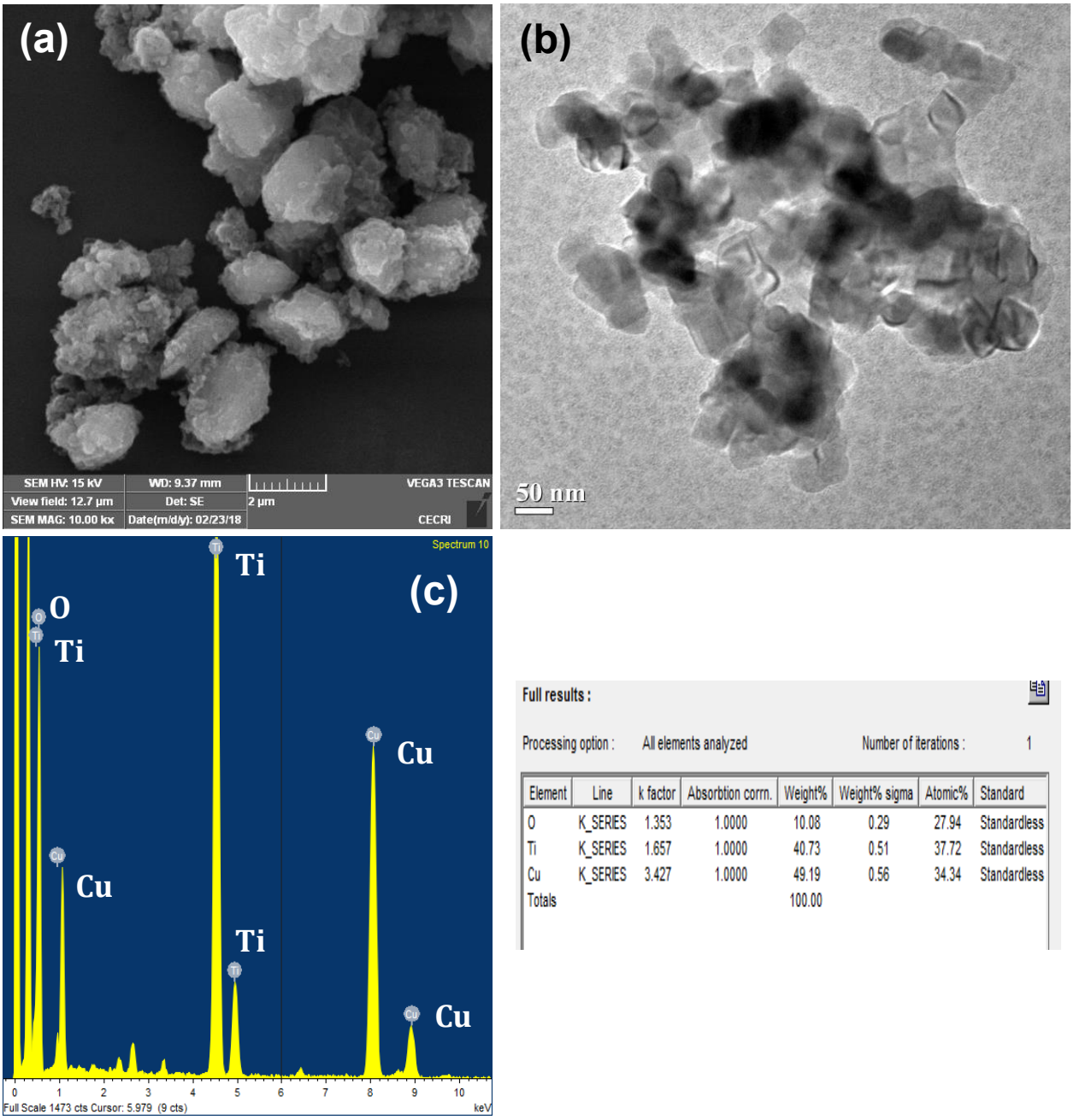

Full results :

Processing option : All elements analyzed Number of iterations : 1

Element	Line	k factor	Absorbtion corrn.	Weight%	Weight% sigma	Atomic%	Standard
O	K_SERIES	1.353	1.0000	10.08	0.29	27.94	Standardless
Ti	K_SERIES	1.657	1.0000	40.73	0.51	37.72	Standardless
Cu	K_SERIES	3.427	1.0000	49.19	0.56	34.34	Standardless
Totals				100.00			

Figure 4. (a) SEM (b) TEM and (c) EDS micrographs of as-synthesized TiO_2 nanomaterial annealed at 800 °C.

The EDS microanalysis was used to confirm the disposition of nanoscale materials. The EDS spectrum (Fig. 4 (c)) shows the characteristic Kα and Kβ peak of titanium (energy of Kα and Kβ: 4.511 keV and 4.931 keV) and the occurrence of a peak at 0.525 keV reveals the presence of O, confirming that the particles in the TEM image are TiO_2 particles. The atomic % of Ti and O is 37.72 and 27.94, respectively. The present compositions of Ti and O in as-synthesised material testify the formation of non-stoichometric TiO_2. Thus, element X-ray spectral mapping identified the chemical make-up of imaged moieties of titanium and oxygen.

Present work report on an easy-to-implement approach for the preparation of TiO_2 nanomaterials from crystalline $[Ti(\eta^5\text{-}C_5H_5)_2(O_2CC_4H_3\text{-}2\text{-}O)_2]$ **3**. Precursor compound **3** is stable towards moisture and can be stored under ambient conditions for months without the need for special protective measures. Unlike extreme moisture sensitive $TiCl_4$ or TTIP, exact dosing of **3** can be manipulated easily for a reaction; a mandatory requirement for reproducibility of the results. Furthermore, the reaction of **3** with water is mild, thus controllable to conduct chemical reactions. Chelating carboxylate and Cp ligands that model coordination environments afford moderately aqueous-stable Ti(IV) complex upon acid treatment. Thus, structurally characterized precursor **3** can be utilized for generation of TiO_2 nanomaterials and the intrinsic pre-regulated structural profile can be correlated/analyzed with the properties/morphologies of resulting TiO_2 nanoparticles.

4. Conclusion

A series of five titanocene complexes of carboxylate ligands, e.g. $[Ti(\eta^5\text{-}C_5H_5)_2(O_2CC_6H_5\text{-}4\text{-}CH_3)_2]$ (**1**), $[Ti(\eta^5\text{-}C_5H_5)_2(O_2CC_4H_3\text{-}2\text{-}O)_2]$ (**2**), $[Ti(\eta^5\text{-}C_5H_5)_2(O_2CC_4H_3\text{-}3\text{-}O)_2]$ (**3**), $[Ti(\eta^5\text{-}C_5H_5)_2(O_2CC(CH_3)_3)_2]$ (**4**) and $[Ti(\eta^5\text{-}C_5H_5)_2(O_2C(CH)C(CH_3)_3)_2]$ (**5**) have been synthesized.

The synthesis of titanocene carboxylates were challenging due to the high oxophilicity of titanium(IV), particularly in the presence of carboxylate ligands. It is worth noting that once the carbonyl oxygen atom is coordinated, the compounds were far less sensitive to nucleophiles such as carboxylate groups or even water, and this stability enables the purification of the compounds. The compounds were characterized by IR, ^{1}H and ^{13}C NMR spectroscopic techniques. An X-ray diffraction study of the synthesized compounds has contributed to the elucidation of the monodentate coordination modes of the carboxylate ligands. To a first approximation, the carboxylate residues were directed away from the Cp rings. Based on C–H…O interactions, usually involving the carbonyl-O atoms, supramolecular chains are found in the crystals of **1**, **4** and **5**, whereas supramolecular layers are found in the crystals of **2** and **3**. Compound **3** was used as precursor for the synthesis of TiO_2 nanoparticles through a wet-chemistry route, which provided softly, agglomerated powders of TiO_2. These were annealed at 800 °C to give TiO_2 nanomaterials with particle sizes in the range between 50-60 nm. The preparation approach could potentially be utilized to incorporate various types of nanomaterials of various sizes, shapes, and compositions. Future work will focus on expanding the applications of this material.

Conflict of interest

The authors declare that they have no conflicts of interest with the contents of this article.

Supplementary material

CCDC 1813139-1813143 contain the supplementary crystallographic data for **1**-**5**, in this order. These data can be obtained free of charge via www.ccdc.cam.ac.uk/getstructures. ESI file contains the figure S1 (a) Digital camera micrograph of $[Ti(\eta^5\text{-}C_5H_5)_2(O_2CC_4H_3\text{-}3\text{-}O)_2]$ (**3**)

stored under an N_2 environment in a Schlenk tube, (b) stereomicroscopic images showing part of surface textures of bulk material of precursor **3**, (c) calcinated TiO_2 nanopowder and (d) TiO_2 nanopowder after ultrasonication and figure S2 (a) PXRD pattern of as-synthesized TiO_2 nanopowder annealed at 400 °C, 600 °C and 800 °C for anatase phase identification and (b) TEM micrographs of as-synthesized TiO_2 nanopowder annealed at 800 °C at 50 K magnification.

Acknowledgements

Financial support from the University Grants Commission, New Delhi (Grant No. Sanction No. 42-396/2013 (SR) Dated 25th March, 2013, TSBB) and the University Grants Commission, New Delhi, India through SAP-CAS, Phase-I (Grant No. F 540/21/CAS/2013 (SAP-I) are gratefully acknowledged. TSBB and RM acknowledge DST-PURSE for the diffractometer facility.

References

[1] (a) D.J. Ramón, M. Yus, *Chem. Rev*., **106**, 2126 (2006); (b) R.O. Duthaler, A. Hafner, *Chem. Rev*., **92**, 807 (1992).

[2] S.A. Ryken, L.L. Schafer, *Acc. Chem. Res*., **48**, 2576 (2015).

[3] (a) E. Le Roux, *Coord. Chem. Rev*., **306**, 65 (2016); (b) V.C. Gibson, S.K. Spitzmesser, *Chem. Rev*., **103**, 283 (2003); (c) L. Resconi, L. Cavallo, A. Fait, F. Piemontesi, *Chem. Rev.*, **100**, 1253 (2000); (d) L. Azor, C. Bailly, L. Brelot, M. Henry, P. Mobian, S. Dagorne, *Inorg. Chem*., **51**, 10876 (2012).

[4] S. Matsuda, A. Kato, *Appl. Catal*., **8**, 149 (1983).

[5] A. Clearfield, D.S. Thakur, *Appl. Catal*., **26**, 1 (1986).

[6] S. Bagheri, N.M. Julkapli, S.B.A. Hamid, *Sci. World J*., (2014), http://dx.doi.org/10.1155/2014/727496. Published Online.

[7] K.P. Bryliakov, E.P. Talsi, *Eur. J. Org. Chem*., **24**, 4693 (2011).

[8] T.R. Helgert, T.K. Hollis, E.J. Valente, *Organometallics*, **31**, 3002 (2012).

[9] (a) M. Albrecht, I. Janser, S. Kamptmann, P. Weis, B. Wibbeling, R. Fröhlich, *Dalton Trans.*, 37 (2004); (b) M. Albrecht, I. Janser, A. Lützen, M. Hapke, R. Fröhlich, P. Weis, *Chem. – Eur. J*., **11**, 5742 (2005); (c) M. Scherer, D.L. Caulder, D.W. Johnson, K.N. Raymond, *Angew. Chem*., **111**, 1689 (1999); (*Angew. Chem*., Int. Ed., **38**, 1587 (1999)); (d) M. Albrecht, H. Röttele, P. Burger, *Chem. – Eur. J*., **2**, 1264 (1996); (e) M. Albrecht, S. Kamtmann, R. Fröhlich, *Polyhedron*, **22**, 643 (2003); (f) M. Albrecht, M. Schneider, R. Fröhlich, *New J. Chem*., **22**, 753 (1998); (g) M. Albrecht, S. Kotila, *Angew. Chem*., **108**, 1299 (1996); *Angew. Chem*., Int. Ed. Engl., **35**, 1208 (1996); (h) Y. Sakata, S. Hiraoka, M. Shionoya, *Chem. –Eur. J*., **16**, 3318 (2010); (i) C. Diebold, P. Mobian, C. Huguenard, L. Allouche, M. Henry, *Inorg. Chem*., **49**,

6369 (2010); (j) D. M. Weekes, C. Diebold, P. Mobian, C. Huguenard, L. Allouche, M. Henry, *Chem. – Eur. J*., **20**, 5092 (2014).

[10] P. Mobian, N. Baradel, N. Kyritsakas, G. Khalil, M. Henry, *Chem. – Eur. J*., **21**, 2435 (2015).

[11] C.W. Schwietert, J.P. McCue, *Coord. Chem. Rev*., **184**, 67 (1999).

[12] (a) K.M. Buettner, A.M. Valentine, *Chem. Rev*., **112**, 1863 (2012); (b) T.B. Parks, Y.M. Cruz, A.D. Tinoco, *Inorg. Chem*., **53**, 1743 (2014).

[13] F. Caruso, M. Rossi, *Mini-Rev. Med. Chem*., **4**, 49 (2004).

[14] T. Schilling, K.B. Keppler, M.E. Heim, G. Niebch, H. Dietzfelbinger, J. Rastetter, A.R. Hanauske, *Invest. New Drugs*, **13**, 327 (1995).

[15] J.H. Toney, T.J. Marks, *J. Am. Chem. Soc*., **107**, 947 (1985).

[16] E. Melendez, *Crit. Rev. Oncol. Hematol*., **42**, 309 (2002).

[17] F. Caruso, M. Rossi, *Metal Ions in Biological System*, Vol. 42: *Metal Complexes in Tumor Diagnostics and as Anticancer Agent*s; A. Sigel, H. Sigel, Eds.; Marcel Dekker, New York, USA (2004).

[18] J.C. Dabrowiak, *Metals in Medicine*, Wiley, West Sussex, UK (2009).

[19] U. Olszewski, G. Hamilton, *Med. Chem*., **10**, 302 (2010).

[20] K. Strohfeldt, M. Tacke, *Chem. Soc. Rev*., **37**, 1174 (2008).

[21] E.Y. Tshuva, D. Peri, *Coord. Chem. Rev*., **253**, 2098 (2009).

[22] G. Ramos, Y. Loperena, G. Ortiz, A. Szeto, J. Vera, J. Velez, J. Morales, D. Morrero, L. Castillo, S. Dharmawardhane, E. Melendez, A.V. Washington, *Anticancer Res*., **34**, 1609 (2014).

[23] L.M. Gao, W. Maldonado, X. Narváez-Pita, J.A. Carmona-Negrón, J. Olivero-Verbel, E. Meléndez, *Inorganics*, **4**, 38 (2016); doi:10.3390/inorganics4040038

[24] E.Y. Tshuva, M. Miller, *Coordination Complexes of Titanium(IV) for Anticancer Therapy*, in *Metallo-Drugs: Development and Action of Anticancer Agents*, Eds. A. Sigel, H. Sigel, E. Freisinger, R.K.O. Sigel, Chapter 8, De Gruyter, Berlin (2018).

[25] (a) D. Pérez-Quintanilla, S. Gómez-Ruiz, Ž. Žižak, I. Sierra, S. Prashar, I. del Hierro, M. Fajardo, Z.D. Juranić, G.N. Kaluđerović, *Chem. Eur. J*., **15**, 5588 (2009); (b) G.N. Kaluđerović, D. Pérez-Quintanilla, I. Sierra, S. Prasar, I. del Hierro, Ž. Žižak, M. Fajardo, S. Gómez-Ruiz, *J. Mater. Chem*., **20**, 806 (2010); (c) A. García-Peñas, S. Gómez-Ruiz, D. Pérez-Quintanilla, R. Paschke, I. Sierra, S. Prashar, I. del Hierro, G.N. Kaluđerović, *J. Inorg. Biochem*., **106**, 100 (2012); (d) J. Ceballos-Torres, P. Virag, M. Cenariu, S. Prashar, M. Fajardo, E. Fischer-Fodor, S. Gómez-Ruiz, *Chem. Eur. J*., **20**, 10811 (2014); (e) W.A. Wani, S. Prashar, S. Shreaz, S. Gómez-Ruis, *Coord. Chem. Rev*., **312**, 67 (2016); (f) S. Gómez-Ruiz, A. García-Peñas, S. Prashar, A. Rodríguez-Diéguez, E. Fischer-Fodor, *Materials*, **11**, 224 (2018); doi:10.3390/ma11020224.

[26] U. Schubert, J. Mater. Chem., **15**, 3701 (2005).

[27] (a) C.-C. Wang, J.Y. Ying, Chem. Mater., **11**, 3113 (1999) (b) Y. Sang, B. Geng, J. Yang, Nanoscale, **2**, 2109 (2010).

[28] K. Sabyrov, N.D. Burrows, R.L. Penn, *Chem. Mater*., **25**, 1408 (2012).

[29] H. Xu, S. Ouyang, P. Li, T. Kako, J. Ye, *ACS Appl. Mater. Interfaces*, **5**, 1348 (2013).

[30] G. Cheng, Y. Wei, J. Xiong, Y. Gan, J. Zhua, F. Xu, *Inorg. Chem. Front*., **4**, 1319 (2017).

[31] H. Wang, H. Lin, Y. Long, B. Ni, T. He, S. Zhang, H. Zhu, X. Wang, *Nanoscale*, **9**, 2074 (2017).

[32] (a) E.A. Gladkikh, T.S. Kuntsevich, *Zh. Strukt. Khim*., **14**, 949 (1973); (b) *J. Struct. Chem.* (Engl. Transl.) **14**, 898 (1973).

[33] D.M. Hoffman, N.D. Chester, R.C. Fay, *Organometallics*, **2**, 48 (1983).

[34] (a) K. Doppert, H. Klein, U. Thewalt, *J. Orgnomet. Chem*., **303**, 205 (1986); (b) R. Leik, L. Zsolnai, G. Huttner, E.W. Neuse, H.H. Brintzinger, *J. Organomet. Chem*., **312**, 177 (1986).

[35] Y. Zhou, Z. Wang, X. Wang, Y. Zhu, *Polyhedron*, **9**, 783 (1990).

[36] (a) F. Xu, Z.-W. Gao, L.-X. Gao, J.-L. Li, *Acta Crystallogr*., **E 62**, m2811 (2006); (b) F. Xu, Z.-W. Gao, C.-Y. Zhang, L.-X. Gao, J.-L. Li, *Acta Crystallogr*., **E 63**, m540 (2007); (c) Z.-W. Gao, F. Xu, C.-Y. Zhang, L.-X. Gao, *Acta Crystallogr*., **E 63**, m542 (2007); (d) J.-L. Li, Z.-W. Gao, L.-X. Gao, F. Xu, *Acta Crystallogr*., **E 63**, m460 (2007); (e) J. Li, Z. Gao, C. Zhang, L. Gao, *J. Chem. Crystallogr*., **39**, 623 (2009).

[37] (a) S. Gómez-Ruiz, B. Gallego, Ž. Žižak, E. Hey-Hawkins, Z.D. Juranić, G.N. Kaluđerović, *Polyhedron,* **29**, 354 (2010); (b) G.N. Kaluđerović, V. Tayurskaya, R. Paschke, S. Prashar, M. Fajardo, S. Gómez-Ruiz, *Appl. Organomet. Chem*., **24**, 656 (2010); (c) S. Gómez-Ruiz, J. Ceballos-Torres, S. Prashar, M. Fajardo, Ž. Žižak, Z.D. Juranić, G.N. Kaluđerović, *J. Organomet. Chem*., **696**, 3206 (2011); (d) J. Ceballos-Torres, M.J. Caballero-Rodríguez, S. Prashar, R. Paschke, D. Steinborn, G.N. Kaluđerović, S. Gómez-Ruiz, *J. Organomet. Chem*., **716,** 201 (2012).

[38] T.C. Stamatatos, S.P. Perlepes, C.P. Raptopoulou, V. Psycharis, N. Klouras, *Polyhedron*, **30**, 451 (2011).

[39] Y. Dang, H.J. Geise, R. Dommisse, E. Esmans, H.O. Desseyn, *J. Organomet. Chem*., **381**, 333 (1990).

[40] Agilent Technologies, *CrysAlisPro*. Santa Clara, CA, USA (2013).

[41] G.M. Sheldrick, *Acta Crystallogr*., **A 64**, 112 (2008).

[42] G.M. Sheldrick, *Acta Crystallogr*., **C 71**, 3 (2015).

[43] L.J. Farrugia, *J. Appl. Crystallogr*., **45**, 849 (2012) .

[44] DIAMOND, *Visual Crystal Structure Information System*, Version 3.1, CRYSTAL IMPACT, Postfach 1251, D-53002 Bonn, Germany (2006).

[45] A.L. Spek, *Acta Crystallogr. Sect. D: Biol. Crystallogr*., **65**, 148 (2009).

[46] K.E. Branham, J.W. Mays, G.M. Gray, R.D. Sanner, G.E. Overturf III, R. Cook, *Appl. Organometal. Chem*., **11**, 213 (1997).

[47] G.B. Deacon, R.J. Philips, *Coord. Chem. Rev*., **33**, 227 (1980).

[48] C.R. Groom, I.J. Bruno, M.P. Lightfoot, S.C. Ward, *Acta Crystallogr. B Struct. Sci. Cryst. Eng. Mater.*, **72**, 171 (2016).

[49] Z. Gao, C. Zhang, M. Dong, L. Gao, G. Zhang, Z. Liu, G. Wang, D. Wu, *Appl. Organometal. Chem*., **20**, 117 (2006).

[50] X. Chen, A. Selloni, *Chem. Rev*., **114**, 9281 (2014), and references therein.

[51] T.J. Boyle, R.P. Tyner, T.M. Alam, B.L. Scott, J.W. Ziller, B.G. Potter Jr., *J. Am. Chem. Soc*., **121**, 12104 (1999).

[52] D. Wang, R. Yu, N. Kumada, N. Kinomura, *Chem. Mater*., **11**, 2008 (1999).

[53] Y.L. Fu, Y.L. Liu, Z. Shi, B.Z. Li, W.Q. Pang, *J. Solid State Chem*., **163**, 427 (2002).

[54] N. Groenke, G. A. Seisenbaeva, V. V. Kaminsky, B. Zhivotovsky, B. Kost, V.G. Kessler *RSC Adv*., **2**, 4228 (2012).

[55] N.Y. Turova, E.P. Turevskaya, V.G. Kessler, M.I. Yanovskaya, *The Chemistry of Metal Alkoxides*, Kluwer, Boston (2002).

[56] G.A. Seisenbaeva, G. Daniel, J.M. Nedelec, V.G. Kessler, *Nanoscale*, **5**, 3330 (2013).

[57] Y.F. Deng, Y.Q. Jiang, Q.M. Hong, Z.H. Zhou, *Polyhedron*, **26**,1561 (2007).

[58] T.J. Boyle, D.T. Yonemoto, T.Q. Doan, T.M. Alam, *Inorg. Chem*., **53**, 12449 (2014).

[59] J. Muscat, V. Swamy, N.M. Harrison, *Phys. Rev*., **B 65**, 224112 (2002).

Table 1. Crystal data and refinement details for compounds **1**-**5**.

Compound	**1**	**2**	**3**	**4**	**5**
Formula	$C_{26}H_{24}O_4Ti$	$C_{20}H_{16}O_6Ti$	$C_{20}H_{16}O_6Ti$	$C_{20}H_{28}O_4Ti$	$C_{22}H_{32}O_4Ti$
Formula weight	448.35	400.21	400.21	380.29	408.37
Crystal colour	Orange	Orange	Orange	Yellow	Yellow
Crystal size/mm^3	0.15 x 0.21 x 0.21	0.12 x 0.15 x 0.15	0.15x 0.19 x 0.19	0.19 x 0.20 x 0.20	0.02 x 0.15 x 0.15
Crystal system	Triclinic	Monoclinic	Monoclinic	Orthorhombic	Triclinic
Space group	$P\bar{1}$	$P2_1/n$	$P2_1/n$	$Cmcm$	$P\bar{1}$
a/Å	8.3000(5)	11.4916(8)	11.1077(11)	11.2217(10)	7.3874(10)
b/Å	10.7348(7)	11.5506(5)	11.0269(11)	14.2341(12)	12.2551(16)
c/Å	13.6735(9)	14.2660(10)	15.2998(13)	13.0839(11)	13.5476(18)
α/°	74.925(6)	90	90	90	74.483(12)
β/°	73.941(6)	112.049(8)	109.396(11)	90	77.300(12)
γ/°	81.339(5)	90	90	90	87.807(11)
V/Å^3	1126.39(13)	1755.1(2)	1767.6(3)	2089.9(3)	1152.6(3)
Z	2	4	4	4	2
D_c/g cm^{-3}	1.322	1.515	1.504	1.209	1.177
F(000)	468	824	824	808	436
μ(Mo$K\alpha$)/mm^{-1}	0.409	0.523	0.519	0.428	0.393
Measured data	8592	8014	7244	3238	9575
θ range/°	3.1 – 28.7	3.1 – 28.7	3.3 – 28.6	3.1 – 28.6	3.2 – 28.6

Unique data	5107	4008	3975	1321	5181
Observed data ($I \geq 2.0\sigma(I)$)	3850	2776	1705	995	2865
No. parameters	282	244	244	69	250
R, obs. data; all data	0.050; 0.128	0.058; 0.138	0.060; 0.096	0.056; 0.130	0.089; 0.178
a; b in weighting scheme	0.070; 0.239	0.065; 0.040	0.025; 0	0.074; 1.187	0.062; 0.634
R_w, obs. data; all data	0.070; 0.144	0.092; 0.152	0.132; 0.152	0.081; 0.146	0.160; 0.212
GoF	1.01	1.08	0.89	1.00	1.08
Range of residual electron density peaks/eÅ^{-3}	-0.33 – 0.43	-0.30 – 0.33	-0.36 – 0.35	-0.25 – 0.26	-0.27 – 0.25

Table 2. Geometric parameters (Å, °) for molecular structures **1**-**5**.

Compound	**Ti–O1, O3**	**Ti–Cg1, Cg2** [a]	**O1–Ti–O3**	**Cg1–Ti–Cg2**	**Cp1/Cp2 dihedral**
1	1.9295(17), 1.9446(18)	2.055(3), 2.0629(18)	90.12(8)	132.28(9)	49.9(3)
2	1.958(2), 1.927(2)	2.0442(19), 2.0553(18)	94.27(10)	131.55(8)	49.7(2)
3	1.935(3), 1.960(3)	2.064(3), 2.068(2)	92.55(13)	130.90(12)	50.6(4)
4 [b]	1.932(2), 1.932(2) [i]	2.0561(19), 2.0561(19) [i]	90.04(16)	132.03(7)	50.65(18)
5	1.934(3), 1.930(3)	2.057(3), 2.057(3)	91.80(14)	131.73(13)	50.6(3)

[a] Cg1 represents the ring centroid of the cyclopentadienyl ring with the lowest C-atom label.

[b] The molecule has crystallographic symmetry (see text). Symmetry operation i: x, y, 1.5 - z.

Table 3. Geometric parameters (Å, °) characterizing intermolecular C–H…O contacts in **1**-**5**.

A	H	B	H···B	A···B	A–H···B	Symmetry operation
1						
C20	H20	O2	2.48	3.296(6)	146	1-x, -y, 1-z
C21	H21	O4	2.44	3.300(5)	155	-x, 1-y, 1-z
C24	H24	O2	2.54	3.444(5)	164	1-x, -y, 1-z
C25	H25	O4	2.36	3.229(4)	155	-x, 1-y, 1-z
2						
C3	H3	O4	2.53	3.336(5)	145	-1/2-x, 1/2+y, 1/2-z
C17	H17	O5	2.58	3.466(5)	159	-1+x, y, z
3						
C3	H3	O2	2.57	3.411(6)	151	1/2-x, 1/2+y, 1/2-z
C13	H13	O4	2.40	3.210(8)	145	3/2-x, -1/2+y, 1/2-z
C17	H17	O4	2.51	3.350(8)	150	3/2-x, -1/2+y, 1/2-z
C20	H20	O2	2.54	3.412(7)	157	1/2-x, 1/2+y, 1/2-z
4						
C7	H7	O2	2.40	3.282(5)	158	x, 1-y, 1-z
5						
C15	H15	O2	2.46	3.369(7)	167	1-x, 1-y, 1-z
C16	H16	O4	2.35	3.265(8)	167	1-x, 2-y, 1-z